

# Design of Multiple Impeller Stirred Tanks for the Mixing of Highly Viscous Fluids Using CFD

Joëlle Aubin\* & Catherine Xuereb

Laboratoire de Génie Chimique UMR CNRS 5503

5 rue Paulin Talabot, BP-1301, 31106 Toulouse Cedex 1, France

Aubin J. and Xuereb C., 'Design of Multiple Impeller Stirred Tanks for the Mixing of Highly Viscous Fluids Using CFD', *Chem. Eng. Sci.*, 61, 2913-2920, (2006).

\*Corresponding author: Dr. Joëlle Aubin, tel: +33-5-34-61-52-43, fax: +33-5-34-61-52-53, email: [Joelle.Aubin@ensiacet.fr](mailto:Joelle.Aubin@ensiacet.fr)

## Abstract

The effect of multiple Intermig impeller configuration on hydrodynamics and mixing performance in a stirred tank has been investigated using computational fluid dynamics. Connection between impeller stages and compartmentalisation has been assessed using Lagrangian particle tracking. The results show that by a rotating Intermig impeller by 45° respect to its neighbours, instead of a 90° rotation as recommended by manufacturers, enables a larger range of operating conditions, i.e. lower Reynolds number flows, to be handled. Furthermore by slightly decreasing the distance between the lower two impellers, fluid exchange between the impellers is ensured down to  $Re = 27$ .

## Keywords

Mixing, Laminar Flow, Hydrodynamics, Homogenisation, Computational Fluid Dynamics, Intermig Impeller

## 1. Introduction

The mixing of highly viscous fluids is a common operation in the chemical, pharmaceutical, biochemical and food industries. Nevertheless, efficient mixing remains a difficult task, as does the design and scale-up of the stirred tank itself. Close clearance impellers such as screws, helical ribbons and anchors are well adapted to the processing of highly viscous liquids; however, they are less efficient when a change in viscosity

occurs throughout the process. For such applications, coaxial stirring systems combining a close clearance agitator with a turbine or axial flow impeller, and also large diameter ratio axial agitators, e.g. Intermig or double-flux impellers, may be more appropriate (Letellier *et al.*, (2002)).

Intermig is an interference multistage counterflow impeller that has an inner pitched blade and an outer double blade arranged in a staggered position with an opposing blade angle. Due to the staggering of the outer blades, interference is produced causing a distinct axial deviation of the flow. As a result, these low-shear axial flow agitators used at large diameter ratios (0.5T-0.95T) are highly suitable for blending, suspending, dispersing, as well as heat transfer applications in both the laminar and transitional flow regimes. Typically, following manufacturers' instructions (EKATO, 1991), Intermigs are installed in pairs, each being rotated 90° respect to one another and are separated vertically by a distance of 0.5T to effectively mix at Reynolds numbers ( $Re$ ) > 100.

Due to their versatility and effective performance for a number of applications in varying flow regimes, it is not surprising that Intermig impellers are readily used in the process industries. However, it appears that there have been very few studies published in the literature that concern the flow and performance of these agitators. Nienow (1990) found that when the inner blades of the Intermig pump downwards in gas-dispersion applications, flooding occurs much more easily than when they are up-pumping. Ibrahim and Nienow (1995) used streak photography to examine the flow patterns produced by a pair of Intermigs and concluded that the flow patterns produced are complex and very different from the schematic diagram given by the manufacturers. They also compared the power curves of the impellers with down-pumping and up-pumping inner blades for laminar through to turbulent flow regimes. The curves coincided for the entire range of  $Re$  and for three values of impeller clearance. More recently, Szalai *et al.* (2004) have analysed the mixing performance of four Intermig impellers (separated by 0.58T) for  $Re = 37, 50, 100$  with experimental and numerical techniques. Using Particle Image Velocimetry (PIV) and Plane Laser-Induced Fluorescence (PLIF), as well as Computational Fluid Dynamics (CFD), it is shown that the flow pattern produced by the Intermig impellers is complex and highly 3-dimensional. The authors found that for low  $Re$ , severe compartmentalization occurs, preventing mixing in the axial direction. It is shown that by varying the agitation rate at periodic intervals, the vertical segregation is broken and mixing at low  $Re$  is improved. This technique had been previously employed for improving the mixing performance in a typical tank configuration stirred with a disc turbine (Yao *et al.*, (1998)).

As discussed by Szalai *et al.* (2004), one of the most challenging tasks in the process industries is the design and scale-up of reactors for processing of highly viscous fluids. Experimental studies are often restricted to the

acquisition of global values, e.g. mixing times, due to the fact that there are not a lot of experimental techniques that allow the measurement of local velocities in high viscosity fluids. The classical techniques, such as Laser Doppler Velocimetry and Particle Image Velocimetry, which enable local measurements, are often limited for use in high viscosity liquids due to the diffusion of the laser beam or sheet. CFD, on the other hand, is not limited by such technological aspects. It can be used a sort of ‘numerical probe’ or sensor to obtain local information about the complex flow field and is therefore an extremely valuable and reliable tool for laminar process design. Nevertheless, efficient methods for characterising complex 3-dimensional laminar flow fields obtained by are still required. Typically, the results of CFD calculations are presented as 2-dimensional velocity vector fields; these however can give completely misleading impressions about the flow. Much work has been done by Muzzio and co-workers concerning the characterisation of complex laminar flow fields (see for example Lamberto *et al.* (1999) or Szalai *et al.* (2004). They quantify mixing efficiency by calculating the stretching intensity of a particle trajectory as a function of position and time. Although their method gives much insight on the complex nature of laminar flows, the computational effort is rather important. With this in mind Harvey III *et al.* (2000) set out to develop a particle-mapping technique to quantify laminar mixing performance in a multiple impeller stirred tank. Their method has enabled the calculation of a ‘mixing time’, which is the time needed for a particle to travel a prescribed distance.

In this study, we focus on the performance of a tank stirred by four Intermig impellers, in terms of hydrodynamics, for viscous fluid processes using CFD. The aim is to determine the operating limitations of a typical configuration of the agitation system, and then to modify the configuration of mixing system so that a wider range of operating conditions can be handled. In order to evaluate the performance of the agitation system, particle trajectories have been calculated and a simple quantitative statistical analysis of the results has been carried out.

## **2. Tank geometry**

The tank geometry employed in the work is a flat bottomed cylindrical tank with a diameter ( $T$ ) set to 1m and the height to diameter ratio ( $H/T$ ) of 2 (Figure 1). The vessel is equipped with four Intermig impellers, diameter ( $D$ ) =  $0.9T$ , which are separated by a distance of  $0.45T$ . The off-bottom clearance of the lowest impeller is  $0.22T$  (distance from the vessel bottom to the lowest impeller swept plane). Three different impeller configurations have been studied. The first case corresponds to a typical installation whereby the Intermig impellers are rotated by  $90^\circ$  with respect to one another. For the second and third configurations, each Intermig

is rotated  $45^\circ$  relative to its neighbours in a clockwise and an anti-clockwise direction, respectively. The impeller rotates at 37 rpm such that the inner blade of the Intermig is down-pumping and the outer fork is up-pumping. Two other modified configurations, whereby the inner blade pumps upwards or the distance between the two lowest impellers is reduced, are then tested. The characteristics of each case are summarized in Table 1.

The model fluid used is Newtonian and has a density of  $1100 \text{ kg.m}^{-3}$ . Three values of viscosity – equal to 9, 15, and 20 Pa.s – have been tested, which correspond to Reynolds numbers of 60, 37 and 27, respectively.

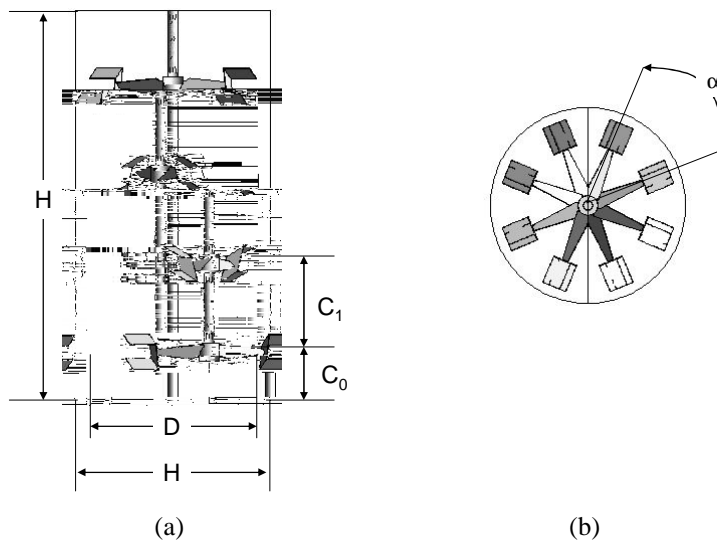


**Figure 1:** Geometry of the vessel equipped with four Intermig impellers. (a) Side view with dimensions, (b) overhead view indicating the relative impeller rotation,  $\alpha$ .

**Table 1:** Summary of the geometrical configurations studied.

Case name	Relative impeller rotation, $\alpha$	Pumping direction of inner blades	Distance separating impellers, $C_1$
IMIG-90	$90^\circ$	Down	0.45T
IMIG-45CW	$45^\circ$ clockwise	Down	0.45T
IMIG-45ACW	$45^\circ$ anti-clockwise	Down	0.45T
IMIG-90-U	$90^\circ$	Up	0.45T
IMIG-45ACW-C	$45^\circ$ anti-clockwise	Down	0.4T for two lowest Intermigs 0.45T for others

### 3. Numerical methods

The numerical simulation of the flow and mixing in the stirred vessel has been performed using ANSYS-CFX5 (ANSYS, 2003). This is a general purpose commercial CFD package that solves the Navier-

Stokes equations using a finite volume method via a coupled solver. The analysis procedure has been carried out in two steps. Firstly the velocity and pressure fields in the tank are solved. These values are then used to calculate particle trajectories with the flow field.

### 3.1 Flow computation

A mesh composed of approximately 1 300 000 elements (300 000 nodes) was used to model half of the vessel, which is geometrically symmetric. A preliminary grid convergence study was carried out in order to verify that the solution is grid independent. No-slip boundary conditions are applied to the vessels walls and the impellers. The free liquid surface is modelled with a zero-flux and zero-stress condition. Since this flow problem involves laminar flow in a stirred tank without baffles, a single rotating reference frame technique has been used. The CFX5.7 solver is used to solve the steady-state momentum and continuity equations for the fluid flow in the tank. The advection terms in each equation were discretised using a bounded second order differencing scheme. The simulations were typically considered converged when the root mean square residuals for all quantities fell below  $1 \times 10^{-6}$ .

### 3.2 Particle tracking

In this study, mass-less fluid particles are followed using a Lagrangian particle tracking method in order analyse the 3-dimensional flow in the tank. The movement of the particle tracers in the flow is determined by integration of the vector equation of motion for each particle:

$$\frac{d\mathbf{x}}{d t} = v(\mathbf{x}) \quad (1)$$

In order to obtain a sufficient degree of accuracy when integrating the equation of motion, a fourth order Runge-Kutta scheme with adaptive step size has been employed. Furthermore, a restitution coefficient of unity is applied to the vessel wall and the impellers. This avoids particle trajectories being trapped near the solid surfaces where the local velocity is close to zero.

### 3.3 Probability of presence

In a perfectly mixed tank over an infinite amount of time, a tracer particle will pass through all points in the tank with an equal probability; this can be assessed by the probability of presence. Barrué *et al.* (1999) used the probability of presence to statistically assess the presence of a particle in a zone of the tank volume. The

probability of presence,  $P$ , of particle  $i$  in zone  $k$  of the tank can be calculated as the time passed in this zone,  $t_{ik}$ , divided by the total trajectory time,  $t_{io}$ :

$$P_{ik} = \frac{t_{ik}}{t_{io}} \quad (2)$$

The total trajectory time is 400 seconds, which corresponds to 246 impeller revolutions. The tank volume has been divided into horizontal slabs, corresponding to compartments created by the flow. The interfaces between two adjacent compartments are situated at horizontal positions  $z = 0.2$  m,  $z = 0.6$  m,  $z = 1.5$  m and  $z = 2.0$  m.

## 4. Results and discussion

### 4.1 Typical configuration: 90° rotation between Intermig stages

The flow field generated by four Intermig impellers (each rotated by 90° relative its neighbours) at  $Re = 60$  is given in Figure 2. These vector plots, each taken at different tangential positions in the tank, show that a complex 3-dimensional flow field is produced, which varies strongly in the azimuthal direction. This confirms the experimental PIV data and CFD simulations presented by Szalai *et al.* (2004). Just above the tip of each impeller a distinct circulation loop forms, while in the centre of the tank there is a predominant downward axial flow. Depending on the azimuthal position of the lowest Intermig, a circulation loop also exists at the bottom of the vessel, whereby the fluid flows down the vessel wall and then up towards the shaft. This loop of course disappears moving towards the impeller plane due to the down-pumping movement of the inner Intermig blades. As the Reynolds number decreases ( $Re = 37$  and  $Re = 27$ ), the circulation loops created by the Intermigs are not as well defined as those shown in Figure 2, although there still appears to be some connection between the impellers (results not shown).

From the vector plots presented in Figure 2, it appears that the circulation loops produced by the four Intermig impellers with 90° rotation are well connected in each impeller plane. However, with such complex 3-dimensional flows, it is difficult to quantify whether the loops really are well connected via the analysis of 2-dimensional data. As a result, it is difficult to interpret whether the axial mixing is adequate and that compartmentalisation is minimal.

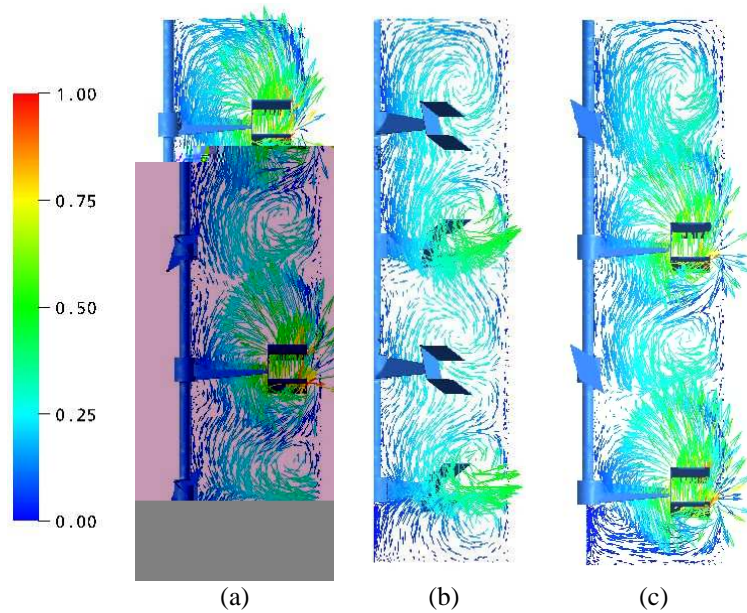


**Figure 2:** Radial-axial flow patterns for IMIG-90 at  $Re = 60$ . (a)-(c) planes varying in the azimuthal direction. Vectors coloured by the velocity normalized by the impeller tip speed ( $1.75 \text{ ms}^{-1}$ ).

To verify whether the flows produced by each Intermig impeller interact, a 3-dimensional analysis of the mixing performance of this configuration is carried out using mass-less tracer particles. Two groups of four particles (one at the height of each impeller) are released simultaneously in the vessel either close to the vessel wall ( $r = 0.45 \text{ m}$ ) or in the bulk flow ( $r = 0.25 \text{ m}$ ).

Figure 3 (a-c) compares the particle traces for  $Re = 60$ ,  $37$  and  $27$ , respectively. Particle tracking time is  $400s$ , which is equivalent to  $246$  impeller revolutions. For  $Re = 60$  (Figure 3 (a)), it can be seen that there are five circulation loops: one above each impeller, as well as one close to the vessel floor. The particle traces show that fluid is exchanged between the four Intermigs, although the connection between the two lower impellers appears to be slightly weaker compared with the upper stages. At  $Re = 37$  (Figure 3 (b)), there appears to be segregation between the lowest Intermig and the upper three impellers: the central part of the lower circulation loop is almost entirely isolated, having minimal exchange with the rest of the vessel. Furthermore, the circulation loop close to the vessel floor is no longer traced, which suggested that it is also isolated at this  $Re$ . At  $Re = 27$  (Figure 3 (c)), it can be seen that the circulation loops in the bulk of the tank are entirely closed, suggesting very poor fluid exchange between the impellers and thus severe compartmentalisation. Only the fluid at the edge of these circulation loops undergoes slow axial convection. There is also evidence of isolated flow regions close to the tank wall, between two main circulation loops.

With the aim of eliminating this compartmentalisation at low Re and extending the operating zone of the stirred tank, the operation and/or setup of the mixing system has been modified as follows.

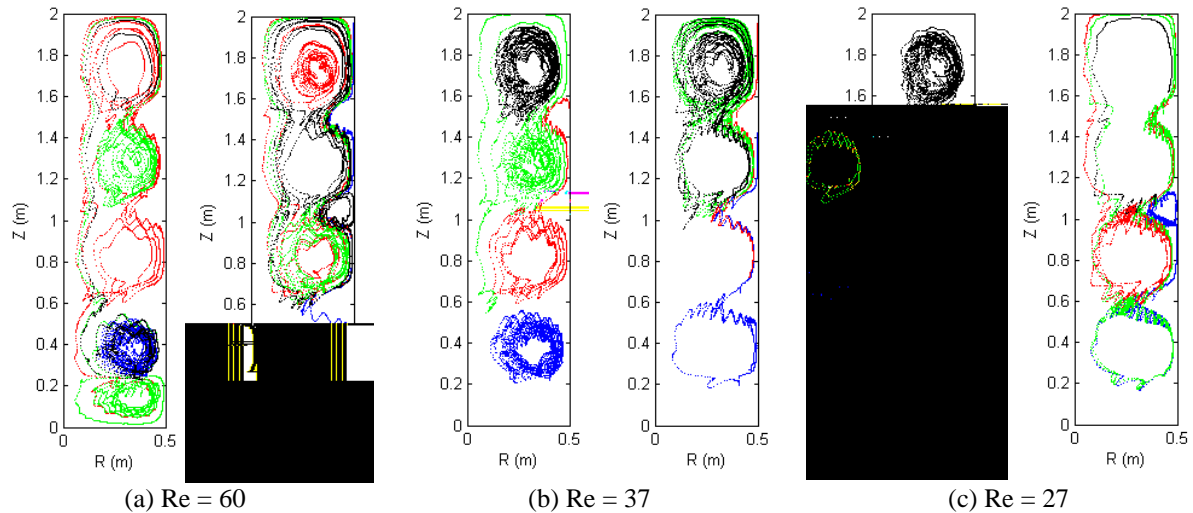


**Figure 3:** 3-dimensional particle tracking projected on to a radial-axial plane for IMIG-90. (a)  $Re = 60$ , (b)  $Re = 37$ , (c)  $Re = 27$ . Particle are released in level with the 4 Intermigs (■  $z = 0.27$  m; ■  $z = 0.72$  m; ■  $z = 1.17$  m, ■  $z = 1.62$  m) and at two radial positions  $r = 0.25$  m (left figure) and  $r = 0.45$  m (right figure).

#### 4.2 Up-pumping versus down-pumping

In order to determine whether the pumping direction of the inner Intermig blades has an effect on axial mixing, the flow produced by up-pumping Intermigs rotated at  $90^\circ$  has been analysed. The radial-axial vector plots (not shown) are similar but opposite to those of the down-pumping configuration, with a predominant up-flowing axial movement in the centre of the vessel. Like for the down-pumping case, the particle tracks for the up-pumping configuration (Figure 4) give evidence of isolated regions with slow axial convection on the outskirts of the circulation loops. Interestingly, the centres of the circulation loops created with the up-pumping impellers are positioned slightly higher in the ves

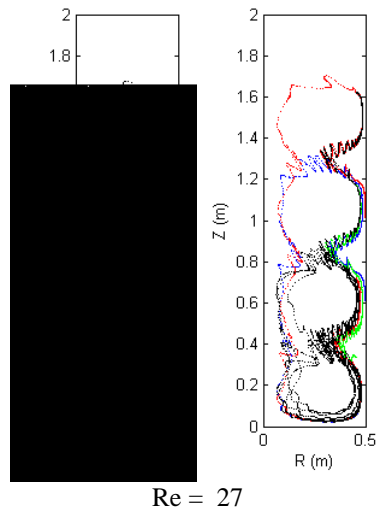


**Figure 4:** 3-dimensional particle tracking projected on to a radial-axial plane for IMIG-90-U at  $Re = 27$ . Particle are released in level with the 4 Intermigs (■  $z = 0.27$  m; ■  $z = 0.72$  m; ■  $z = 1.17$  m, ■  $z = 1.62$  m) and at two radial positions  $r = 0.25$  m (left figure) and  $r = 0.45$  m (right figure).

#### 4.3 Effect of a $45^\circ$ rotation between Intermig stages

Knowing that the pumping direction does not improve the fluid exchange between the impellers at low  $Re$ , the impellers are rotated by  $45^\circ$  clockwise or anti-clockwise so that the impeller configuration resembles a spiral staircase. For these configurations, the circulation loops are well established and the vectors (not shown) suggest that there is good fluid exchange between the Intermig impellers. Figures 5 and 6 shows particle tracks for both the  $45^\circ$  clockwise and anti-clockwise relative impeller rotation, respectively for  $Re = 60, 37$  and  $27$ . Overall it appears that the direction in which the Intermigs are rotated relative to one another (clockwise or anti-clockwise) does not influence the interference behaviour. The power consumption (Table 2), however, is slightly lower for the anti-clockwise rotation, being equivalent to the typical  $90^\circ$  configuration. For  $Re = 60$ , there is fluid exchange between the four impeller stages, with a slightly weaker connection between the two lower Intermigs. The performance is similar to that of the typical configuration. At  $Re = 37$ , there is still adequate connection between the four upper circulation regions, which suggests better axial mixing than for the configuration with  $90^\circ$  rotation. When the  $Re$  is lowered to  $27$ , the  $45^\circ$  configurations still ensure fluid exchange between the upper three Intermig impellers, with compartmentalisation of only the lowest Intermig.

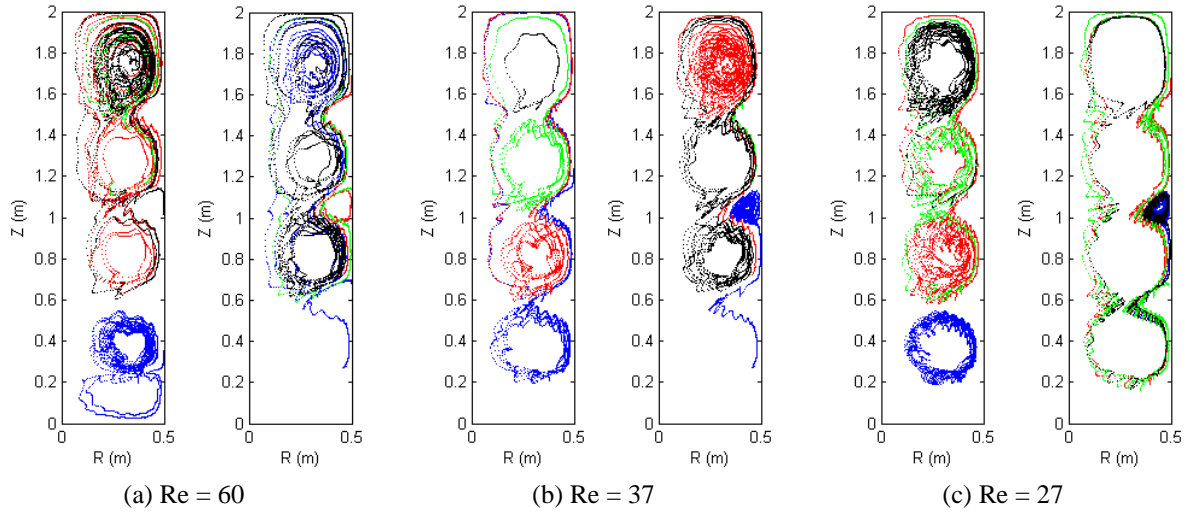


**Figure 5:** 3-dimensional particle tracking projected on to a radial-axial plane for IMIG-45CW. (a) Re = 60, (b) Re = 37, (c) Re = 27. Particle are released in level with the 4 Intermigs (■  $z = 0.27$  m; ■  $z = 0.72$  m; ■  $z = 1.17$  m, ■  $z = 1.62$  m) and at two radial positions  $r = 0.25$  m (left figure) and  $r = 0.45$  m (right figure).

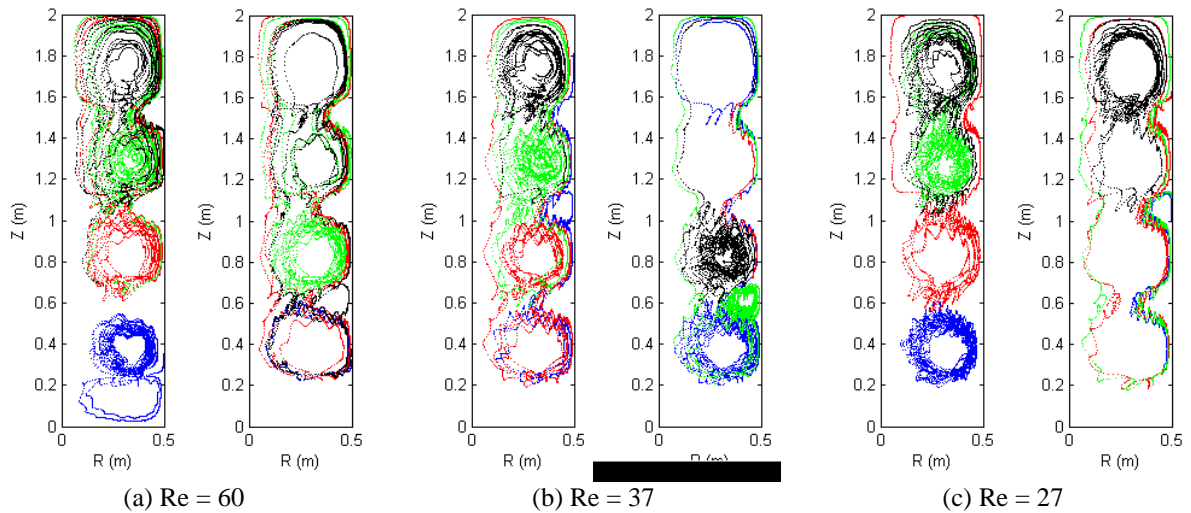


**Figure 6:** 3-dimensional particle tracking projected on to a radial-axial plane for IMIG-45ACW. (a) Re = 60, (b) Re = 37, (c) Re = 27. Particle are released in level with the 4 Intermigs (■  $z = 0.27$  m; ■  $z = 0.72$  m; ■  $z = 1.17$  m, ■  $z = 1.62$  m) and at two radial positions  $r = 0.25$  m (left figure) and  $r = 0.45$  m (right figure).

In order to improve the flow connection between the lowest Intermig and the upper three impellers at Re = 27, the distance between the lower two Intermigs of the 45° anti-clockwise rotation case was decreased slightly from 0.45T to 0.4T (the distance separating the other impellers remained at 0.45T). The corresponding particle tracks are shown in Figure 7. It can be seen that this slight decrease in distance enables re-connection between the

lowest Intermig and the upper three impellers stages and therefore better axial mixing, without decreasing the convection in the upper part of the vessel or increasing power consumption (Table 2).

**Table 2:** Comparison of  $N_p \cdot Re$  for the various cases studied for  $Re = 60, 37$  and  $27$ .

	$N_p \cdot Re$		
	$\mu = 9 \text{ Pa}\cdot\text{s}, Re = 60$	$\mu = 15 \text{ Pa}\cdot\text{s}, Re = 37$	$\mu = 20 \text{ Pa}\cdot\text{s}, Re = 27$
<b>IMIG-90</b>	266	230	215
<b>IMIG-45CW</b>	271	235	220
<b>IMIG-45ACW</b>	265	229	214
<b>IMIG-90-U</b>	—	—	215
<b>IMIG-45ACW-C</b>	—	—	214

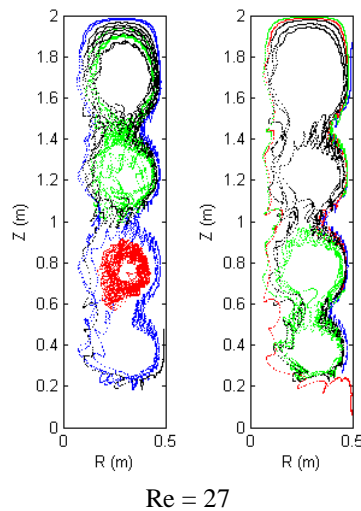


**Figure 7:** 3-dimensional particle tracking projected on to a radial-axial plane for IMIG-45ACW-C at  $Re = 27$ . Particle are released in level with the 4 Intermigs (■  $z = 0.27 \text{ m}$ ; ■  $z = 0.72 \text{ m}$ ; ■  $z = 1.17 \text{ m}$ , ■  $z = 1.62 \text{ m}$ ) and at two radial positions  $r = 0.25 \text{ m}$  (left figure) and  $r = 0.45 \text{ m}$  (right figure).

#### 4.4 Probability of presence

The probability of presence of the particle tracers has been calculated for the four down-pumping geometries for a Reynolds number of 27. The results, presented as histograms in Figure 8, depict the percentage of total travelling time that a particle has spent in a particular zone. Ideally, considering the non-equal volumes of the defined zones, one would expect the particle to spend 10% of its time in zone 0-0.2 m, 20% in each of zones 0.2-0.6 m and 0.6-1.0 m, and 25% in both of zones 1.0-1.5 m 1.5-2.0 m.

In the top graph of Figure 8(a) it can be seen that three of the particles released at  $r = 0.25$  m spend 100% of their trajectory time in the zone where they were released. When the particles are released closer to the vessel wall, however, they have more of a tendency to change circulation zones. For these conditions, there is zero probability that a particle enters the zone close to the vessel floor, as shown by the particle traces in the previous figures. Looking at Figures 8(b-c), it can be seen that by positioning the impellers at  $45^\circ$  to one another, the compartmentalization observed in the case of the IMIG-90 is greatly reduced, especially for the particles released at  $r = 0.25$  m. When the distance between the lower two impellers decreases, the improvement in the flow exchange between zones, shown in Figure 7, is confirmed by the histograms in Figure 8(d). Excluding the zone close to the vessel floor, the time spent by each particle in each compartment is more evenly distributed than that found for the other three geometries, especially for the particles released at  $r = 0.25$  m.

#### *4.5 Inter-compartmental exchange*

The histograms in Figure 8 present the cumulative residence time of a particle in each of the defined zones but does not indicate the frequency that a particle changes compartment. Table 3 shows the average period (1/frequency) of inter-compartmental exchange of a particle. Zero value indicates that the particle did not move zones during the entire trajectory time.

Looking closely at the results, it can be seen that by decreasing the rotational distance between two impellers to  $45^\circ$ , compared with  $90^\circ$ , the inter-compartment flow exchange is improved and the exchange frequency is generally increased. The difference between the IMIG-45CW and IMIG-45ACW cases is more subtle, but the ACW case is marginally better overall. The improvement of inter-compartmental exchange with the case IMIG-45ACW-C is striking. For this case, the particles change zone about every 20 seconds, corresponding to approximately 12 impeller revolutions, which is at least twice as fast as most of the particles in case IMIG-45ACW.

**Table 3:** Comparison of the average time period needed for a particle to change compartments.

Case	Average Period of Inter-Compartmental Exchange (s)							
	Particle Release Position							
	r = 0.25m				r = 0.25m			
	z = 0.27m	z = 0.72m	z = 1.17m	z = 1.62m	z = 0.27m	z = 0.72m	z = 1.17m	z = 1.62m
IMIG-90 Re = 27	—	—	—	113	136	64	31	29
IMIG-45CW Re = 27	—	82	45	55	199	18	19	37
IMIG-45ACW Re = 27	93	40	59	40	46	19	24	39
IMIG-45ACW-C Re = 27	15	90	24	26	20	19	19	16

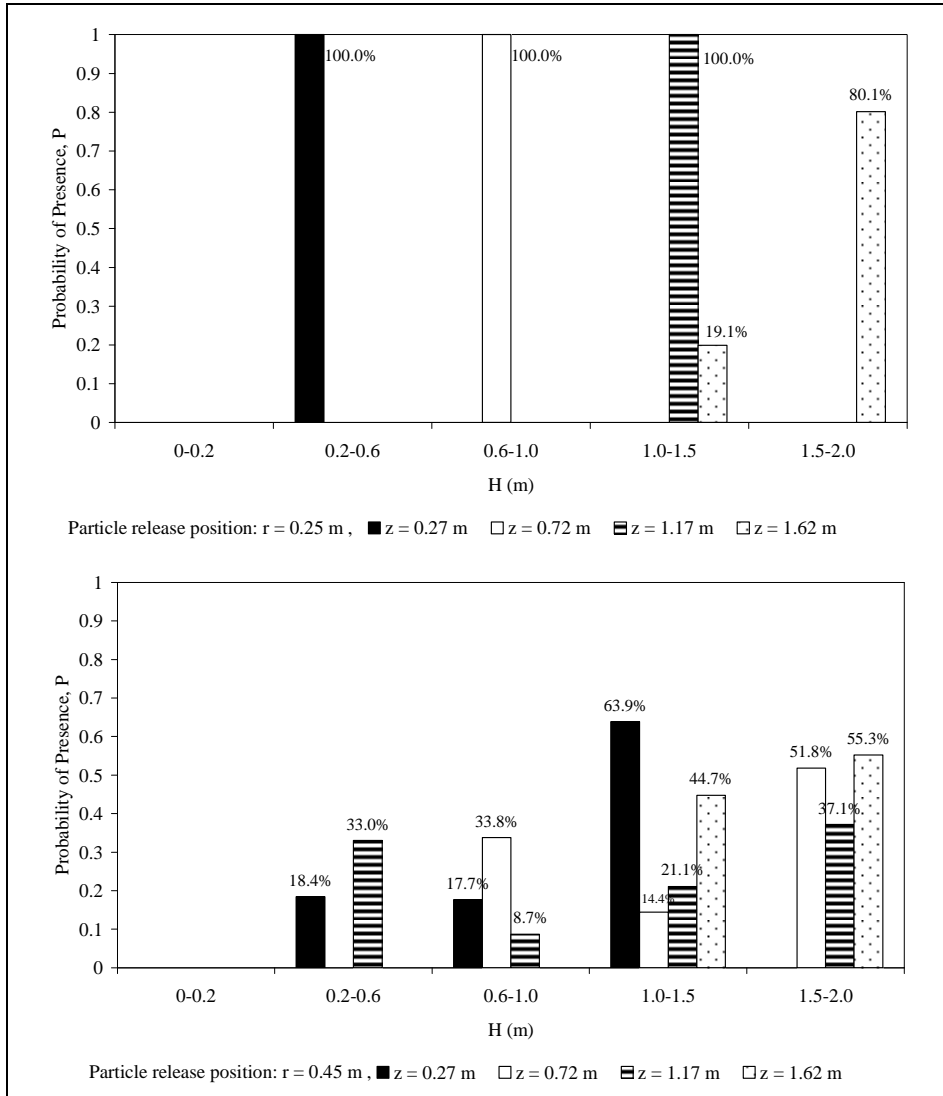
## 5. Conclusions

The laminar flow and mixing in a tank stirred by four Intermig impellers has been studied and analysed using CFD. The performance of a typical configuration of the agitation system, whereby the impellers are rotated at 90° with respect to one another, is compared with impeller systems rotated by 45°. The flow produced by Intermig impellers has been shown to be highly complex and 3-dimensional. As a result, 2-dimensional vector fields can be misleading when evaluating the hydrodynamics and mixing in such stirred tanks. A 3-dimensional analysis using Lagrangian particle tracking has been found to better describe the interaction between the impeller stages. In addition, a statistical analysis has been used to quantify the probability that a particle is in a particular zone of the tank and the frequency that the particle changes zones. Using these analysis tools, it has been shown that compartmentalisation occurs at  $Re < 60$  for a typical Intermig system with 90° rotation between impellers. By simply rotating the impellers by 45° respect to one another to form a spiral staircase, the connection and fluid exchange between the impeller stages is improved. As a result, Reynolds numbers down to 37 can be handled before vertical segregation occurs with no increase in power consumption. Finally it has been shown that the range of operating conditions can be further enlarged by slightly decreasing the distance between the lower two Intermig impellers from 0.45T to 0.4T. This configuration ensures fluid exchange between the impellers down to at least  $Re = 27$ .

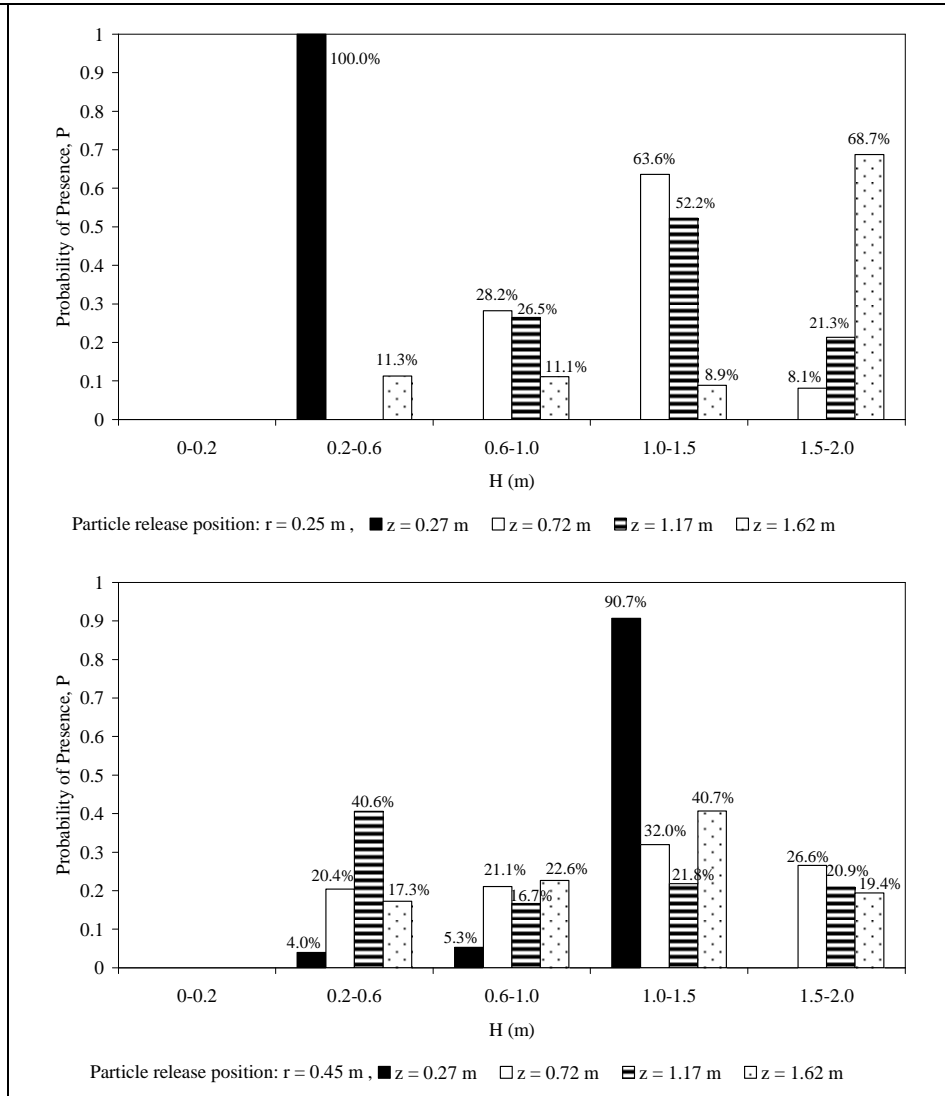
Future work will involve the experimental study of the geometries presented here to evaluate the mixing time as well as the zone exchange frequency and the residence time of a tracer in each compartment. In addition, modifications to the geometrical configuration will be carried out to prevent compartmentalization in the bottom of the tank.

## References

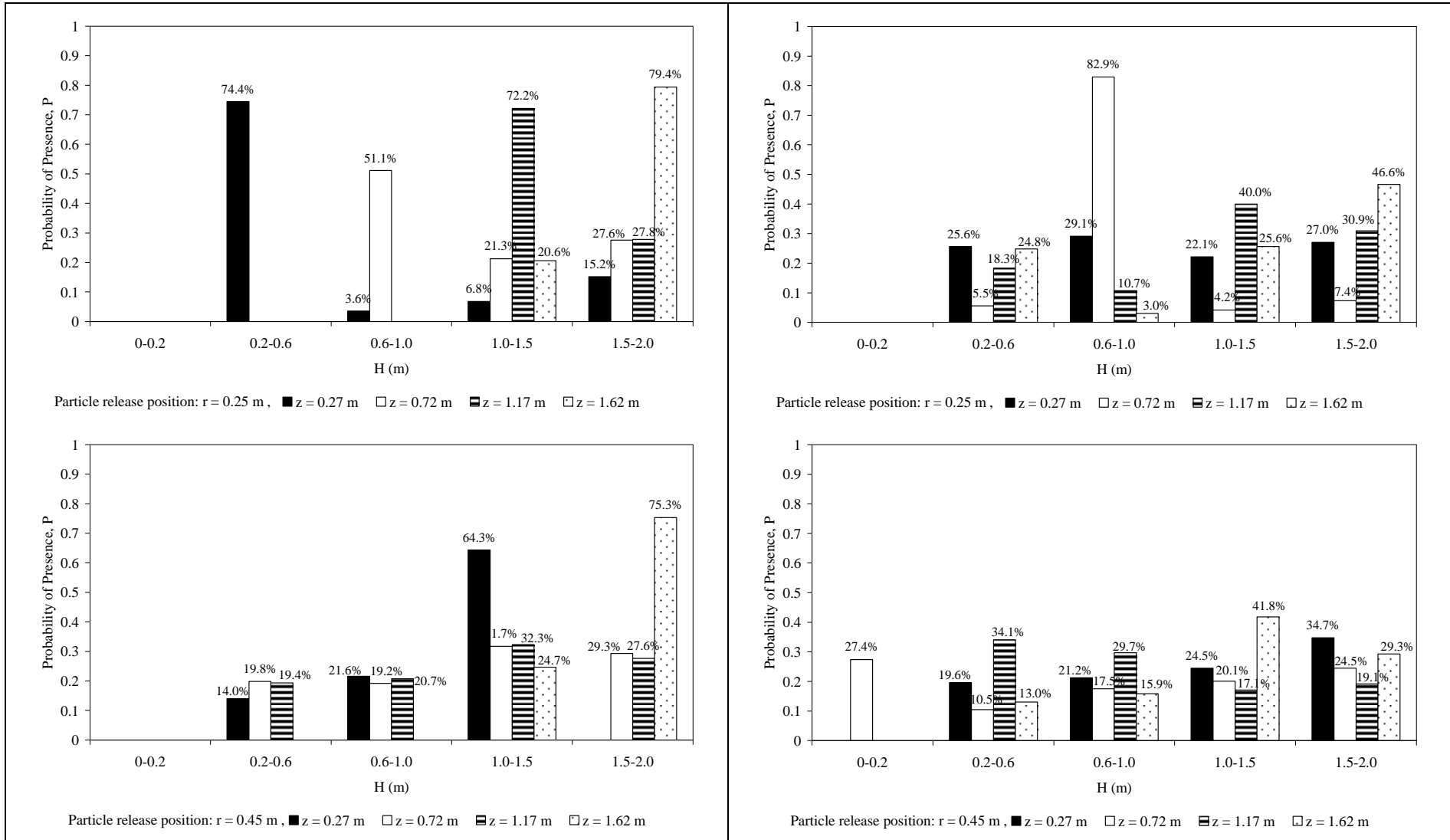
- Barrué, H., Xuereb, C., Pitiot, P., Falk, L. and Bertrand, J., (1999). Comparison of Experimental and Computational Trajectories in a Stirred Vessel. *Chemical Engineering & Technology*, 22, 511-521.
- EKATO, (1991). *Handbook of Mixing Technology: General Theory, Selection Criteria, Application*. EKATO Rühr-und Mischtechnik GmbH, Schopfheim.
- Harvey III, A.D., West, D.H. and Tufillaro, N.B., (2000). Evaluation of Laminar Mixing Using a Discrete-Time Particle-Mapping Procedure. *Chemical Engineering Science*, 55, 667-684.
- Ibrahim, S. and Nienow, A.W., (1995). Power Curves and Flow Patterns for a Range of Impellers in Newtonian Fluids:  $40 < Re < 5 \times 10^5$ . *Transactions of the Institution of Chemical Engineers*, 73(A), 485-491.
- Lamberto, D., Alvarez, M.M. and Muzzio, F.J., 1999. Experimental and Computational Investigation of the Laminar Flow Structure in a Stirred Tank. *Chemical Engineering Science*, 54, 919-942.
- Letellier, B., Xuereb, C., Swaels, P., Hobbes., P. and Bertrand, J., (2002). Scale-up in Laminar and Transient Regimes of a Multi-stage Stirred, a CFD approach. *Chemical Engineering Science*, 57, 4617-4632.
- Nienow, A.W., (1990). Gas Dispersion Performance in Fermenter Operation. *Chemical Engineering Progress*, February, 61-71.
- Szalai, E.S., Arratia, P., Johnson, K. and Muzzio, F.J., (2004). Mixing Analysis in a Tank Stirred with Ekato Intermig Impellers. *Chemical Engineering Science*, 59, 3793-3805.
- Yao, W.G., Sato, H., Takahashi, K. and Koyama, K., (1998). Mixing Performance Experiments in Impeller Stirred Tanks Subjected to Unsteady Rotational Speeds. *Chemical Engineering Science*, 53, 3031-3040.



(a) IMIG-90,  $Re = 27$



(b) IMIG-45CW,  $Re = 27$



(c) IMIG-45ACW, Re = 27

(d) IMIG-45ACW-C, Re = 27

**Figure 8:** Probability of presence of tracer particles to be found in a particular compartment. (a) IMIG-90, Re = 27, (b) IMIG-45CW, Re = 27, (c) IMIG-45ACW, Re = 27, (d) IMIG-45ACW-C, Re = 27